Climate
of the Past

Open Access

Northward advection of Atlantic water in the eastern Nordic Seas over the last 3000 yr

C. V. Dylmer[1], **J. Giraudeau**[1], **F. Eynaud**[1], **K. Husum**[2], and **A. De Vernal**[3]

[1]Université de Bordeaux, CNRS, UMR5805 EPOC, Talence, France
[2]Department of Geology, University of Tromsoe, Tromsoe, Norway
[3]GEOTOP, Université du Québec à Montréal, Montréal, Canada

Correspondence to: C. V. Dylmer (c.dylmer@epoc.u-bordeaux1.fr)

Abstract. Three marine sediment cores distributed along the Norwegian (MD95-2011), Barents Sea (JM09-KA11-GC), and Svalbard (HH11-134-BC) continental margins have been investigated in order to reconstruct changes in the poleward flow of Atlantic waters (AW) and in the nature of upper surface water masses within the eastern Nordic Seas over the last 3000 yr. These reconstructions are based on a limited set of coccolith proxies: the abundance ratio between *Emiliania huxleyi* and *Coccolithus pelagicus*, an index of Atlantic vs. Polar/Arctic surface water masses; and *Gephyrocapsa muellerae*, a drifted coccolith species from the temperate North Atlantic, whose abundance changes are related to variations in the strength of the North Atlantic Current.

The entire investigated area, from 66 to 77° N, was affected by an overall increase in AW flow from 3000 cal yr BP (before present) to the present. The long-term modulation of westerlies' strength and location, which are essentially driven by the dominant mode of the North Atlantic Oscillation (NAO), is thought to explain the observed dynamics of poleward AW flow. The same mechanism also reconciles the recorded opposite zonal shifts in the location of the Arctic front between the area off western Norway and the western Barents Sea–eastern Fram Strait region.

The Little Ice Age (LIA) was governed by deteriorating conditions, with Arctic/Polar waters dominating in the surface off western Svalbard and western Barents Sea, possibly associated with both severe sea ice conditions and a strongly reduced AW strength. A sudden short pulse of resumed high WSC (West Spitsbergen Current) flow interrupted this cold spell in eastern Fram Strait from 330 to 410 cal yr BP. Our dataset not only confirms the high amplitude warming of surface waters at the turn of the 19th century off western Svalbard, it also shows that such a warming was primarily induced by an excess flow of AW which stands as unprecedented over the last 3000 yr.

1 Introduction

The late Holocene was governed by a cooling trend known as the neoglaciation (Porter and Denton, 1967). Compared with the preceding early to mid-Holocene climate optimum, the neoglaciation has been widely recorded in both terrestrial and marine archives in the North Atlantic region (Jennings et al., 2002; Seidenkrantz et al., 2008; Kaufman et al., 2009, and references herein; Andresen et al., 2011; Müller et al., 2012) as a time of expansion of Scandinavian glaciers (Nesje et al., 1991, 2001), increased sea ice cover and colder surface waters in the Barents Sea and part of Fram Strait (Duplessy et al., 2001; Risebrobakken et al., 2010; Kinnard et al., 2011; Müller et al., 2012), colder surface and subsurface waters off western Norway (Calvo et al., 2002; Moros et al., 2004; Hald et al., 2007; Sejrup et al., 2011) and overall colder conditions over northern Europe (Bjune et al., 2009). This cooling trend was punctuated by several warm and cold spells such as the Roman Warm Period and Medieval Climate Anomaly (RWP, MCA), and the Little Ice Age (LIA). Over the last century, the LIA was reversed by an overall increase in temperature, as seen in, terrestrial high resolution proxy records of the Arctic region (Overpeck et al., 1997; Kaufman et al., 2009) and proxy records from marine sediment cores of the northern North Atlantic (Spielhagen et al., 2011; Hald et al.,

2011; Wilson et al., 2011). Marine proxy-based reconstructions suggest that this recent temperature increase in the subsurface layer west of Spitsbergen (Spielhagen et al., 2011) and in shallow settings off Northwest Norway (Hald et al., 2011) were unprecedented over the past two millennia. Both studies implied that this warming was probably caused by enhanced advection of Atlantic Water (AW) to the Arctic Ocean during modern times, although none were able to strictly infer the dynamical history of AW, i.e., the history of the strength of the North Atlantic Current (NAC).

The hypothesis of an increased AW inflow during the modern period was further supported by Wanamaker et al. (2012) based on living and fossil molluscan remains north of Iceland; these authors additionally related known pre-Anthropocene warm (MCA) and cold (LIA) climatic spells of the last ∼ 1500 yr to modulations of the surface Atlantic-derived water dynamics within the North Atlantic. This modulation was further evidenced off Florida, at the inception of the Gulf Stream, by Lund et al. (2006) who estimated a 10 % decrease in the flow of this current at the transition from the MCA to the LIA. Similarly, in the nearby Chesapeake Bay, such modulations were also evidenced by Cronin et al. (2005) who linked this to North Atlantic Oscillation (NAO) forcing of sea surface temperature in the western North Atlantic.

The processes controlling variations in the meridional flow of the NAC to the Nordic Seas and ultimately to the Arctic Ocean are either associated with anomalies in the location and strength of the westerlies, and/or changes in the thermohaline circulation (Müller et al., 2012). At present the most prominent pattern of atmospheric variability in the North Atlantic region is known as the NAO, itself depending on the Northern Hemisphere annular mode, the Arctic Oscillation (e.g., Marshall et al., 2001). The NAO is defined as the wintertime difference in atmospheric pressure (sea level) between the Icelandic low and the Azores high, controlling the strength and direction of westerly winds, storm tracks across the North Atlantic, temperature and precipitation over western Europe, and the strength of the poleward NAC and equatorward EGC (East Greenland Current; Blindheim et al., 2000; Hurrell et al., 2003). A low NAO index (reduced westerly flow across the Atlantic) induces a reduced flow of the NAC, less precipitation in northern Europe and a more southern direction of the storm tracks (Hurrell et al., 2003). Whereas a high index favors a strengthened NAC flow, stronger precipitation and an eastward shift of the Arctic front (AF) which separates Atlantic from Arctic waters (ArW), toward the slope off Norway (Blindheim et al., 2000). Furthermore modern observations indicate a significant correlation between the NAO indexes and the Barents Sea ice extent, with less sea ice during the positive NAO (warm) phases and conversely more ice during negative NAO (cold) phases (Vinje, 2001; Sorteberg and Kvingedal, 2006), possibly related to variations in southwesterlies, air masses and Atlantic inflow (Blindheim et al., 2000).

Paleorecords from Arctic Canada and Iceland suggest that a series of explosive volcanism centered at the MCA–LIA transition might have triggered an extensive sea ice expansion during the LIA (Miller et al., 2012). A combined switch in NAO patterns from a long-term positive phase during the MCA to negative NAO conditions during the LIA (Trouet et al., 2009) possibly further enhanced the severe increase in sea ice extent, as decadal and long-term variations in large-scale ice concentrations have shown to be significantly correlated with long-term NAO variations (Visbeck et al., 2003).

However, although the importance of the NAO on the modern hydrography and climate of the Nordic Seas is now well established, assessing its significance on paleoceanographical changes of this ocean realm has long been hampered by the lack of instrumental records prior to the 19th century, and by proxy- and model-based reconstructions reaching back only one millennia (Trouet et al., 2009). A high resolution reconstruction of NAO variability from a lake record in southwestern Greenland (Olsen et al., 2012), recently extended the NAO record back to 5200 yr before present (BP), offering a way to investigate links between atmospheric processes and ocean circulation changes over the mid to late Holocene in the northern North Atlantic.

The NAC impact on the hydrological and climatic changes in the Nordic Seas and the Arctic Ocean is enormous, hence the need for an increased understanding of inflow variations, forcing mechanisms and the consequences on the global climate system is crucial in order to fully understand the changes in our present and future climate.

Previous water column and surface sediment investigations of extant and fossil remains (coccoliths) of coccolithophorids suggested that this species group could be used as proxies, though mostly qualitative, of both water mass distribution and flow strength of the NAC in the northern North Atlantic (Samtleben and Schröder, 1992; Baumann et al., 2000; Schröder-Ritzrau et al., 2001). Andrews and Giraudeau (2003), and Giraudeau et al. (2010) thereafter tested these coccolith proxies to infer the Holocene history of AW flow within the Denmark Strait and across the Iceland–Scotland Ridge. The present manuscript lies on these exploratory works in applying selected coccolith proxies on a set of marine sedimentary cores distributed along the continental margins off western Norway, the western Barents Sea and western Spitsbergen. Our aim is to investigate late Holocene changes in AW flow and associated surface hydrological fronts along the main axis of heat and salt transfer to the Arctic Ocean, which is carried by the NAC and its northernmost extension (West Spitsbergen Current, WSC). Given the major influence of NAO related atmospheric processes on the modern NAC dynamics and climate of the Nordic Seas region, we will thoroughly discuss our proxy results in view of available NAO paleoreconstructions over the last 3000 yr, as well as to nearby terrestrial and marine records.

2 Oceanography

The study area lies as a south–north transect along the continental slope off western Norway, the western Barents Sea and west of Svalbard (Fig. 1). This area is mainly influenced by three water masses; AW, Polar water (PW) and coastal water. Warm (7–13 °C) and saline (≥ 35 PSU) AW is advected north by the NAC (Hopkins, 1991), originating from the Iceland–Scotland Ridge, the main passageway of oceanic salt and heat transfer to the Nordic Seas (ca. 7 Sv; Hansen and Østerhus, 2000). This topographically steered poleward flow of AW splits off northern Norway into a meridional branch, the WSC and a zonal component, the North Cape Current (NCaC). The WSC flows along the slope of the western Barents Sea and off western Svalbard, joined on its northern path by ArW on the shelf from the Bear Island Current (extension around Bjørnøya of the Persey Current, PC) and the Sørkapp Current (extension around southern Svalbard of the East Spitsbergen Current, ESC) (Saloranta and Svendsen, 2001; Wassman et al., 2006) (Fig. 1), and transmits a volume of roughly 3–5 Sv of AW to the Arctic Ocean, part of it being recirculated at intermediate depth below the southward flowing East Greenland Current. North of Svalbard, AW enters the Arctic Ocean as a subsurface current insulated from the atmosphere by fresh PW in the upper mixed layer (Blindheim and Østerhus, 2005). The NCaC transmits 1.8 Sv of AW to the Barents Sea around northern Norway (Skagseth et al., 2008), preventing winter sea ice to develop in the southern region of the Barents shelf. The Norwegian Coastal Current (NCC), flowing along the Norwegian coast is influenced by freshwater runoff from the Norwegian mainland and from the Baltic Sea, and is therefore characterized by reduced salinities (34.4 ∼ PSU) (Wassman et al., 2006).

Sea ice and fresh water from the Arctic Ocean are essentially transmitted to the Nordic Seas via the Fram Strait and the southward flowing cold and fresh EGC (< 0 °C, < 34.5 PSU) (Buch, 1990), the largest and most concentrated meridional ice flow in the world oceans (Blindheim and Østerhus, 2005) (Fig. 1). The northeast–southwest trending boundary between PW and ArW is termed the Polar front indicating the minimum drift ice extent (summer), whereas the boundary between ArW and AW is known as the AF and represents the maximum drift ice extent (winter) (Baumann et al., 2000; Wassman et al., 2006). Though showing some complex local peculiarities, the interannual changes in sea ice extent are closely controlled by atmospheric processes acting over the Nordic Seas and surrounding areas. A link with NAO was proposed by Hurrell (1995) and is consistent with anomalies of sea ice extent in the Barents Sea (Vinje, 2001). Further north in the Greenland Sea, maximum ice export from the Arctic Ocean through the Fram Strait characterizes positive NAO periods (Kwok et al., 2004).
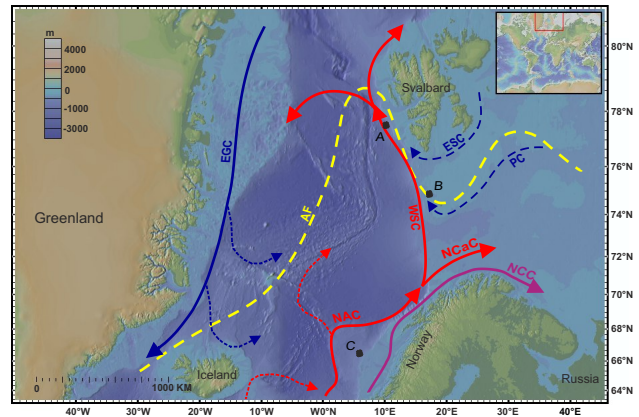

Fig. 1. Bathymetric map of the Nordic Seas showing the major oceanic features and site locations. Red arrows: flow direction of warm saline Atlantic water (NAC: North Atlantic Current, NCaC: North Cape Current, WSC: West Spitsbergen Current), blue arrows: flow direction of cold low salinity Arctic/Polar waters (EGC: East Greenland Current, ESC: East Spitsbergen Current, PC: Persey Current), purple arrow: flow direction of coastal surface current (NCC: Norwegian Coastal Current). Dashed yellow line: modern distribution of the Arctic front (AF). Core locations A: HH11-134-BC (west of Spitsbergen), B: JM09-KA11-GC (western Barents Sea) and C: MD95-2011 (Vøring Plateau).

3 Material and methods

Three marine sediment cores distributed along the Norwegian, Barents Sea, and Svalbard continental margins were specifically selected for the present work (Fig. 1, Table 1).

The southernmost site (hereafter referred to MD95-2011), representing a splice between a box-core (30 cm) covering the top 560 yr (JM97-948/2A) and the MD95-2011 piston core (Giraudeau et al., 2010), was retrieved on the Vøring Plateau off western Norway, located below the main path of the poleward flowing NAC. The present investigation was conducted on the top 220 cm of the composite MD95-2011. The 383 cm long gravity core JM09-KA11-GC, of which the top 25 cm is presented here, was retrieved from the Kveithola Trough, representing the western Barents Sea component of the transect, influenced both by the WSC and Arctic/Polar waters circulating clockwise around Svalbard (Sørkapp Current) and Bjørnøya (Bear Island Current). The 41 cm long box-core HH11-134-BC was retrieved on the West Spitsbergen margin under the axis of the WSC inflow to the Arctic Ocean. The present study was carried out on the top 27 cm of this core.

3.1 Core chronology

The chronologies of the studied sediment core intervals are based on 22 AMS (Accelerator Mass Spectrometry) [14]C- and ^{210}Pb-dates of which 13 have previously been published for cores JM09-KA11-GC (Rüther et al.,

Table 1. Core location, water depth, length and geographical area.

Core ID	Latitude	Longitude	Water depth (m)	Core length (m)	Location
MD95-2011	66°58.19′ N	7°38.36′ E	1048	7.45	Mid-Norwegian margin (Vøring Plateau)
JM97_948/2A BC	66°58.19′ N	7°38.36′ E	1048	0.30	
JM09-KA11-GC	74°52.489′ N	17°12.210′ E	345	3.6	Western Barents Sea (Kveithola Trough)
HH11-134-BC	77°35.96′ N	9°53.25′ E	1383	0.41	West Spitsbergen slope

2012), and MD95-2011 (Risebrobakken et al., 2003) (Table 2). The dates were calibrated to calendar years BP (present = 1950 AD) applying the software Calib 6.1.0 (Stuiver and Reimer, 1993) and the marine calibration curve marine09 (Reimer, 2009) using a reservoir correction of ∼ 400 yr ($\Delta R = 0$). This reservoir correction was chosen as a further fine-tuning of the signals and would result in age models differing from published paleoclimate datasets using the standard variations. Nevertheless we are aware of a possible shift of our age models due to the ΔR effect, especially in areas with "old" Arctic/Polar waters.

The chronologies were established using the calibrated mean ages for the 2σ interval of highest probability and assuming a constant sedimentation rate between each radiocarbon dated level of JM09-KA11-GC (linear interpolation) and a second order polynomial fit for core HH11-134-BC (Fig. 2). The sedimentation rates of the three studied cores range from 5 to 146 cm kyr^{-1}, which according to the sampling resolution, lead to a temporal resolution of our micropaleontological dataset of 10 to 105 yr. A decadal to multi-decadal resolution has been found sufficient in the present study to identify major centennial-scale changes in paleocirculation along our transect.

3.2 Micropaleontological analyses

The sample preparation for the coccolith study was conducted according to the "Funnel" method described by Andruleit (1996). It involves dilution and filtration of a preweighed amount of dry bulk sediment on membrane filters, mounting between slide and coverslip, and examination under a light microscope at × 1000 magnification. A total of more than 300 specimens were counted in order to ensure the statistical reliability of our results (Andruleit, 1996) and were ultimately expressed in terms of relative abundances (species percentage) and absolute concentrations (specimens/gram of dry bulk sediment). Previous repeated analyses of fine fraction sediment samples using the "Funnel" method revealed that the method can cause ∼ 15 % deviation in the bulk coccolith absolute concentrations (Herlle and Bollmann, 2004) and consequently species-specific absolute concentrations. Hence only relative abundances and "major" (≫ 15 % deviation) absolute concentration changes will be addressed in the following.
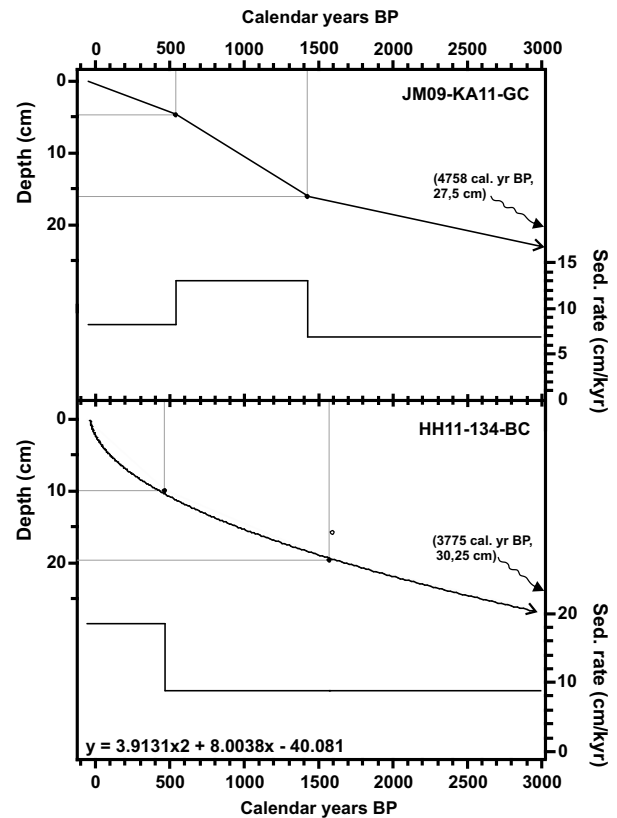

Fig. 2. Calendar age–depth model and sedimentation rates of JM09-KA11-GC (linear interpolation between each dated level) and HH11-134-BC (second order polynomia), based on data from Table 2. Filled circles: include AMS C[14] datings, hollow circles: exclude AMS C[14] datings. The stratigraphic framework of core MD95-2011 was developed by Birks and Koç (2002), Risebrobakken et al. (2003) and Andersson et al. (2003).

An additional investigation on planktonic foraminiferal assemblages was conducted on the northernmost sediment core (HH11-134-BC). Samples were wet sieved through a 63 μm mesh. Counting was performed on the > 100 μm fraction according to Husum and Hald (2012) in order to include smaller size species, which are frequent in assemblages of the northern North Atlantic. We will only present here the relative abundance of subpolar planktic foraminifera, expressed as the sum of *Globigerinata* species and *Turborotalia quinqueloba*.

Table 2. Core, sample depth, dated material, ^{14}C AMS age years BP, calibrated years BP, Laboratory ID and Reference.

Core	Core depth (cm)	Dated material	14C AMS age yr BP	Calibrated age, cal yr BP	Calibrated ages, 2σ range	Lab ID	Reference
HH11-134-BC	9.75	Bulk planktic foraminifera	826 ± 23	462.5	420-505	UBA-20062	
HH11-134-BC	15.5*	Bulk planktic foraminifera	2030 ± 30	1602	1515–1688	SacA 29428	
HH11-134-BC	19.5	Bulk planktic foraminifera	1995 ± 28	1571	1473–1669	UBA-20061	
HH11-134-BC	30.25	Bulk planktic foraminifera	3825 ± 30	3774.5	3676-3873	SacA 29432	
JM09-KA11-GC	4.50	*Bathyarca glacialis*	925 ± 30	543	482–604	TRa-1063	Rüther et al. (2012)
JM09-KA11-GC	16.00	*Bathyarca glacialis*	1880 ± 35	1424.5	1332–1517	TRa-1065	Rüther et al. (2012)
JM09-KA11-GC	27.50	*I*. Norcrossi/ helenae	4430 ± 30	4758	4745–4771	Beta-324049	Berben et al. (2013) and Groot et al. (2013)
JM09-KA11-GC	33*	*A. elliptica*	1990 ± 35	1556	1441–1671	Tra-1066	Rüther et al. (2012)
JM09-KA11-GC	40.00	*I*. Norcrossi helenae	5480 ± 30	5838.5	5749–5928	Beta-315192	Berben et al. (2013) and Groot et al. (2013)
JM97_948/2A BC	4.75			−1		210Pb Dated	Risebrobakken et al. (2003)
JM97_948/2A BC	7.75			18		210Pb Dated	Risebrobakken et al. (2003)
JM97_948/2A BC	10.25			29		210Pb Dated	Risebrobakken et al. (2003)
JM97_948/2A BC	21.75	*N. pachyderma (dex)*	735 ± 40	375.5	290–461	KIA 6285	Risebrobakken et al. (2003)
JM97_948/2A BC	30.75	*N. pachyderma (dex)*	940 ± 40	553.5	485–622	KIA 4800	Risebrobakken et al. (2003)
MD95-2011	10.5	*N. pachyderma (dex)*	980 ± 60	573	489–657	GifA 96471	Risebrobakken et al. (2003)
MD95-2011	30.5	*N. pachyderma (dex)*	1040 ± 40	602.5	534–671	KIA 3925	Risebrobakken et al. (2003)
MD95-2011	47.5	*N. pachyderma (dex)*	1160 ± 30	709.5	650–769	KIA 5601	Risebrobakken et al. (2003)
MD95-2011	70.5	*N. pachyderma (dex)*	1460 ± 50	1021	907–1135	KIA 3926	Risebrobakken et al. (2003)
MD95-2011	89.5	*N. pachyderma (dex)*	1590 ± 30	1148.5	1060–1237	KIA 6286	Risebrobakken et al. (2003)
MD95-2011	154	*N. pachyderma (dex)*	2335 ± 25	1953	1868–2038	KIA 2037	Risebrobakken et al. (2003)
MD95-2011	170.5	*N. pachyderma (dex)*	2620 ± 60	2298	2128–2468	GifA 96472	Risebrobakken et al. (2003)
MD95-2011	269.5	*N. pachyderma (dex)*	3820 ± 35	3768.5	3659–3878	KIA 10011	Risebrobakken et al. (2003)

* Excl. from age model.

3.3 Rationale for the selection of species-specific coccolith proxies

While an overall presentation of the coccolith assemblages in the sediment cores is provided in the present paper, a focus is made on species-specific coccolith proxies of surface water mass distribution and AW flow dynamics in the studied geographical domain.

Extant populations of coccolithophorids thriving in the Nordic Seas are overwhelmingly dominated by *Emiliania huxleyi* (high- to very-high cell densities) and *Coccolithus pelagicus* (medium–high cell densities) (Baumann et al., 2000), with rare occurrences of a few representatives of *Syracosphaera* spp. and of the deep-thriving species *Algirosphaera robusta* (Samtleben and Schröder, 1992; Samtleben et al., 1995). Both *E. huxleyi* and *C. pelagicus* dominate settling assemblages and assemblages in the sediment (Schröder-Ritzrau et al., 2001 and reference herein). *E. huxleyi* is a summer blooming ubiquitous species with a strong affinity for Atlantic-derived surface waters in the eastern part of the Nordic Seas. Beside its preferential distribution within areas bathed by the NAC, this species is suggested to be influenced mainly by variations in stratification, irradiance and to a lesser extent temperature of the photic layer (Samtleben and Schröder, 1992; Samtleben et al., 1995; Baumann et al., 2000; Beaufort and Heussner, 2001).

Coccolithus pelagicus, the cold end-member of the extant coccolithophorid populations in the Nordic Seas, thrives preferentially in the vicinity of the Arctic front and in the Greenland Sea (Samtleben et al., 1995). Turbulence might be an important factor to prevent sinking of this heavily calcified species from the photic zone and therefore favors its dominance in areas with moderate gradients in salinity and temperature (Cachão and Moita, 2000) and/or Arctic to Polar waters.

The different regional dominance of these two species is also reflected in surface sediments (Samtleben et al., 1995). The abundance ratio between *E. huxleyi* and *C. pelagicus* (E / C ratio) in fossil assemblages in the Nordic Seas has therefore been proposed by Baumann et al. (2000) to define the location of the AF, which separates the seasonally ice-covered waters of the Polar and Arctic domains (E / C < 1) from warmer and saltier Atlantic-derived waters (E / C > 1). According to Baumann et al. (2000), the E / C ratio is based on a conversion of coccolith to coccosphere units; the average number of coccoliths per coccosphere for each species is taken from Samtleben and Schröder (1992).

Although the original work by Baumann et al. (2000) were confined to the central areas of the Nordic Seas, we believe the application of this method to be valid in the wider Nordic Seas including its eastern part. The published surface sediment sample dataset by Baumann et al. (2000) only included a few sites far west of the continental margin with coccolith

assemblages dominated by *C. pelagicus* (E / C < 1). This excess *C. pelagicus* abundance stands as a contrast to our own results from surface sediment assemblages in the northern cores HH11-134-BC and JM09-KA11-GC, as well as to the composition of extant populations northwest of Bjørnøya (Baumann et al., 2000) and across the Fram Strait (Dylmer et al., 2013), which both indicate an expected clear dominance of *E. huxleyi* below and within AW dominated areas. Based on these evidences we use the definition of the AF (a frontal salinity and temperature gradient separating surface AW masses from mixed ArW) to infer that the E / C ratio (ie. deviations from the threshold of 1) characterizes surface sediments deposited below Atlantic or Arctic surface water masses, when considering pluriannual conditions.

Though barely found in modern plankton communities of the Nordic Seas (Andruleit, 1997; Dylmer et al., 2013), coccoliths of *Gephyrocapsa muellerae* and *Calcidiscus leptoporus* commonly contribute together up to ∼ 20 % of the fossil assemblages in surface sediments of the eastern Nordic Seas. Drifting with the poleward flow of surface to intermediate NAC waters from the temperate North Atlantic, where these species are preferentially thriving, was proposed as a possible explanation for this discrepancy by Samtleben and Schröder (1992). Based on new datasets on living and fossil communities, Giraudeau et al. (2010) revisited the distributional pattern of *G. muellerae* in the North Atlantic and restricted the ecological niche of this species to the eastern North Atlantic, south of the Iceland–Scotland Ridge. Given this ecological background, abundance changes of *G. muellerae* in the studied sediment cores will be discussed in terms of relative variations of the depth integrated flow strength of the NAC to the Nordic Seas up to its northernmost extension off western Svalbard (WSC).

Even though the mechanism of poleward transport, as described here for *G. muellerae,* is supposed to affect all species thriving in southern latitudes within the path of the NAC, it is not expected to hamper the paleorecords of the high in situ production of the dominating species (e.g., *E. huxleyi* and *C. pelagicus*) in the Nordic Seas, which is transferred to the sediment surface within weeks by fecal pellets (Samtleben and Schröder, 1992; Andruleit, 1997).

4 Results and interpretation

4.1 Bulk coccolith concentrations

Preservation of coccolith remains was good to moderate throughout the three studied cores, hereby confirming the overall relatively good preservation of calcareous microfossils in recent sediments of the eastern Nordic Seas (Hebbeln et al., 1998; Matthiessen et al., 2001). Bulk coccolith concentrations throughout the investigated time interval range from $25 \pm 10 \times 10^8$ specimens g^{-1} of dry sediment (sp g^{-1} dry sed) in the Vøring Plateau area, to a
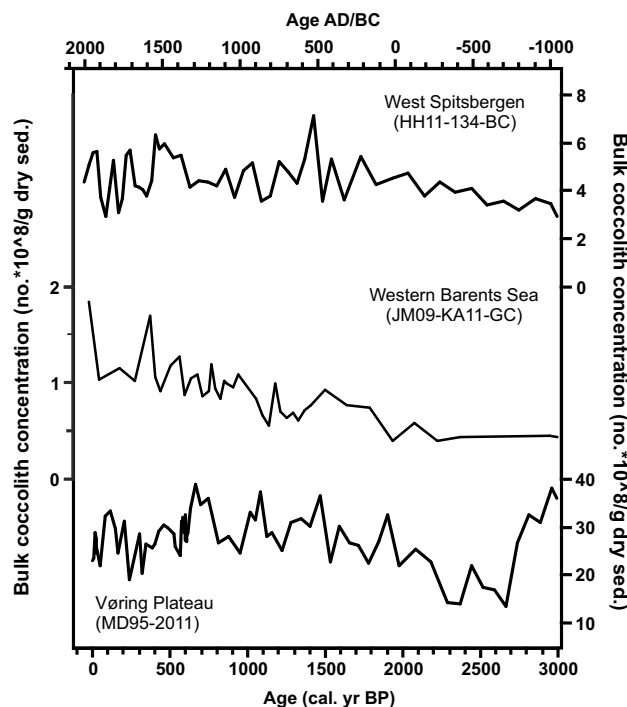

Fig. 3. Bulk coccolith concentration records (coccoliths $\times 10^8$ g^{-1} dry sed).

minimum of $1 \pm 0.5 \times 10^8$ sp g^{-1} dry sed in the Kveithola Trough region (Fig. 3). These values fall within the range of typical coccolith concentrations in surface sediments of the eastern Nordic Seas and accurately reproduce the decreasing poleward trend of coccolith absolute concentrations in sediments presently accumulating along the path of the NAC and WSC (Baumann et al., 2000). While down-core bulk coccolith concentrations are rather stable over the last 3000 yr (with the exception of a short low centered at 2500 cal yr BP) at the Vøring Plateau site, the two northernmost locations off western Barents Sea and Svalbard are characterized by increased values towards the present. Relative changes in the amount and temperature of Atlantic-derived surface waters that sustain most of the calcareous plankton production in the Nordic seas (Schröder-Ritzrau et al., 2001; and references herein) are supposed to explain to a high extent the observed latitudinal and temporal changes in bulk coccolith accumulation (Andruleit and Baumann, 1998). The inferred sedimentation rates in the three studied cores falls within the range of previous investigations carried out in the western Barents sea (Sarnthein et al., 2003), off western Spitsbergen (Werner et al., 2011), and at the Vøring Plateau (Sejrup et al., 2011). The late Holocene sedimentation rates show large variations in-between the studied locations, which can only be explained by geographical differences in terrigenous inputs from nearby continental shelves and/or distribution of sediment-laden sea ice (Vinje et al., 2001; Divine and Dick, 2006). Spatial and temporal changes in dilution of the
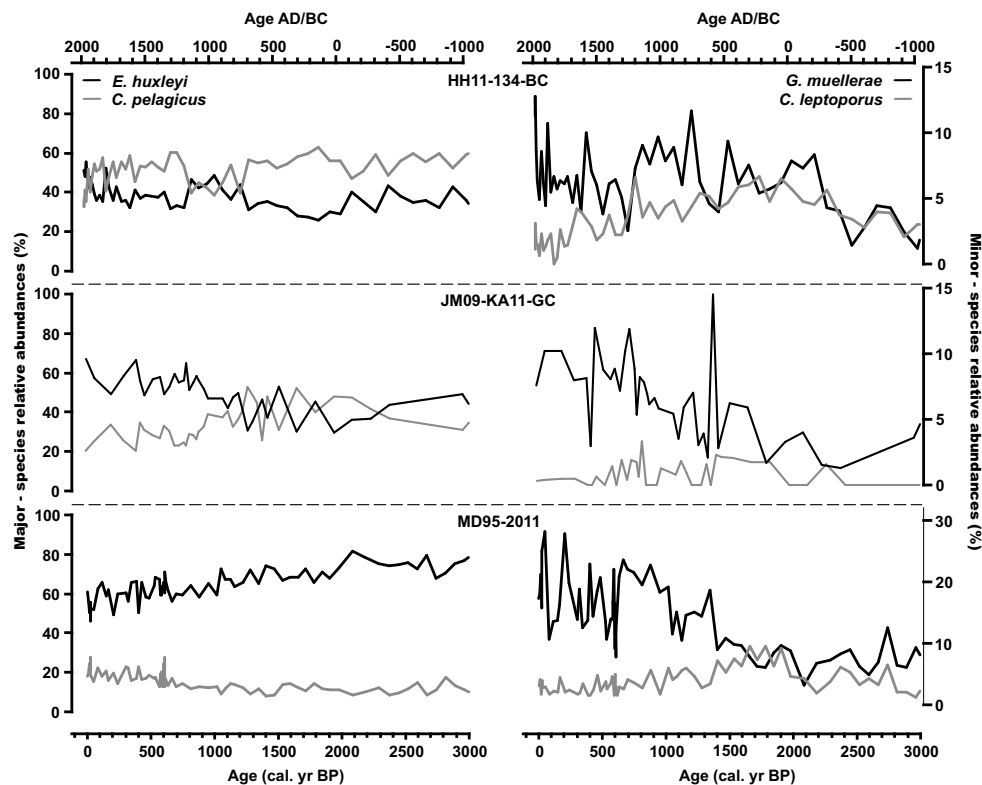
Fig. 4. Relative abundances (%) of major (left axes) and minor (right axes) coccolith species throughout the three studied cores.

biogenic component of Nordic Seas sediments by terrigenous material are consequently likely to bias the significance of bulk coccolith concentration records in terms of paleoproductivity patterns.

4.2 Species assemblages

Coccolith species diversity is typically low as expected for this Arctic/sub-Arctic setting (e.g., Baumann et al., 2000; Matthiessen et al., 2001). The dominance is shared between *C. pelagicus* and *E. huxleyi* in sediments of the two northernmost cores HH11-134-BC and JM09-KA11-GC whereas the latter species always contributes to > 50 % of the total assemblages over the last 3000 yr off Norway (MD95-2011) (Fig. 4). The clear latitudinal shift in dominance from *E. huxleyi* to *C. pelagicus*, which is related to the specific water masses dominating at the core sites (AW/ArW), shows distinct local/regional patterns along the transect with relative abundance changes in the range of 26–56 % (*E. huxleyi*) and 33–63 % (*C. pelagicus*) west of Spitsbergen, 30–67 % and 20–54 % in the western Barents Sea, and 46–82 % and 8–28 % west of Norway. An overall increased *E. huxleyi* contribution interrupted by several millennial-scale low amplitude changes characterizes the west-Spitsbergen core over the studied time interval, with a short shift in dominance weakly apparent in the interval ∼ 1200–800 cal yr BP and more clearly in modern times. The western Barents Sea cores

show an intermediate signal with relatively high *E. huxleyi* abundances toward the beginning and the end of the records and a sustained low between ∼ 1200 and 2300 cal yr BP. West of Norway, although always dominating the coccolith assemblages, *E. huxleyi* displays a steady decreasing abundance from 3000 cal yr BP to the present.

As expected given its overall shared dominance with *E. huxleyi*, *C. pelagicus* displays opposite patterns of relative abundance in all cores.

The resultant E/C ratios show lower values with higher latitudes, ranging from 6.6 to 0.2 (Fig. 5). This ratio displays overall increasing values west of Svalbard and in the western Barents Sea from 3000 yr onward, with a contrasting decreasing trend west of Norway. Increased ratios characterize the early part of the three records from ca. 3000 to 2100 cal yr BP, followed by a period of decreased values between 2100 and 1200 cal yr BP. Thereafter, both HH11-134-BC and JM09-KA11-GC share common patterns with higher species ratios until ∼ 700 cal yr BP, followed by a 600 yr long interval of lower E/C values, and ending with high ratios over the last century. Contrary to the pattern displayed at the two northernmost sites, the species ratios at MD95-2011 show a marked steadily decreasing trend from 1200 cal yr BP to the present.

The subordinate species *G. muellerae* and *C. leptoporus* together account for an average 7.5% of the total assemblage
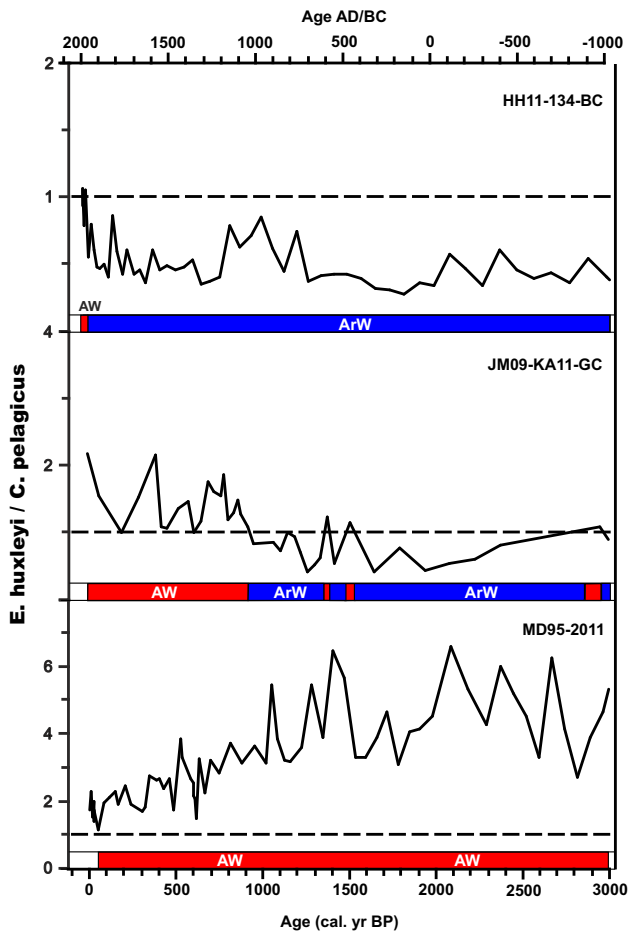
Fig. 5. E / C ratios of the dominant coccolithophore species *E. huxleyi* (E) and *C. pelagicus* (C). The bar charts below each E / C plot highlight the dominating surface water masses at the core locations according to the "1" threshold: blue represents ArW (E / C < 1); red represents AW (E / C > 1).

throughout the studied cores (Fig. 4). A fifth species, *Syracosphaera* sp., only contributes on average 1.8 %, and will not be discussed further.

Contrary to *E. huxleyi* and *C. pelagicus*, the relative abundance changes of the drifted species *G. muellerae* and *C. leptoporus* are characterized by similar general trends along the whole latitudinal transect (Fig. 4).

All sites display an overall increase of *G. muellerae* abundances during the last 3000 yr punctuated by a low steady level in the 3000–2200 cal yr BP interval, a period of highest abundances from ca. 2200 to ~ 650 cal yr BP, followed by marked lower values until the beginning of the last century. With the exception of the southernmost core MD95-2011, *G. muellerae* reaches high abundances in the top-most samples (ca. last 100 yr) off western Svalbard and the western Barents Sea. The trends in absolute concentrations and relative abundances of this drifted species are nearly identical at all studied sites (Fig. 6). Short- and/or long-term changes in sedimentation of sea ice or continental-margin-derived lithic
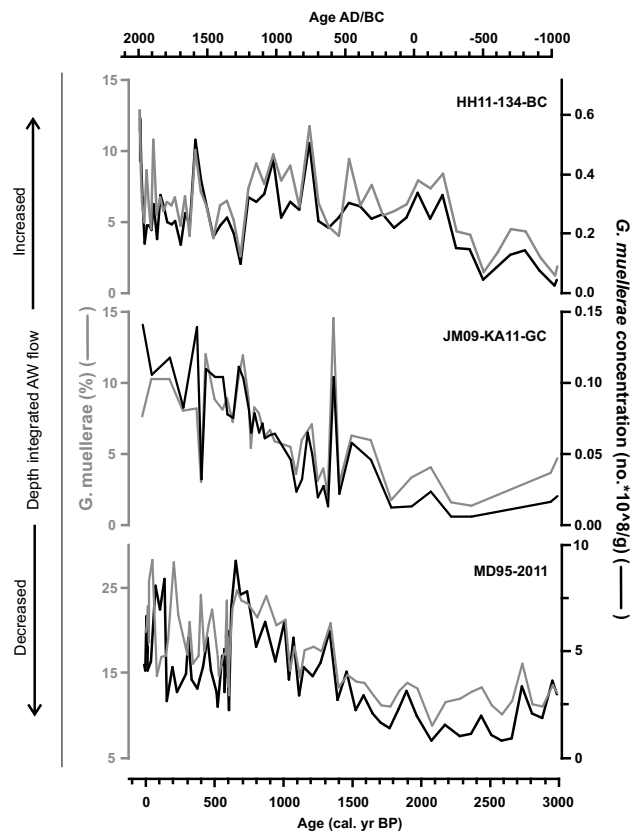

Fig. 6. Relative abundances (grey line) and absolute concentrations (black line) of the AW inflow species *G. muellerae*, throughout the three studied cores. The MD95-2011 record is a late Holocene zoom of previously published data by Giraudeau et al. (2010).

material, which most probably affect patterns of microfossil concentration records, including coccoliths, had therefore no obvious influence on *G. muellerae* absolute abundance trends along the studied transect. Hence *G. muellerae* absolute concentration records can be considered as significant proxies for relative changes in the NAC strength.

C. leptoporus shows a peak in relative abundance within all studied cores (though more than twice lower than the maximum values of *G. muellerae*) centered at ~ 1800–2000 cal yr BP (2–10 %) (Fig. 4). This abundance pattern, different from the other drifted species *G. muellerae*, is enigmatic given the common processes (i.e., poleward transport to the Nordic Seas) affecting both species. One explanation might lay in the less restricted ecological niche of *C. leptoporus* which presently colonizes a wider geographic domain in the North Atlantic from warm to cool temperate areas (i.e., Ziveri et al., 2001) than *G. muellerae* (Giraudeau et al., 2010).

4.3 Variability in the strength of the North Atlantic Current and fluctuations of the Arctic front

Our coccolith records are indicative of important changes in the strength of the NAC and in the dominating surface waters (Arctic vs. Atlantic) within the eastern Nordic Seas over the last 3000 yr. Figure 7 summarizes the main paleoceanographic information inferred from our coccolith proxies, together with the abundance record of subpolar planktonic foraminifera in the northernmost studied core. Both the HH11-134-BC foraminiferal abundance record (this study, Fig. 7) and planktonic foraminiferal stable isotopes and species abundances measured in core MD95-2011 (Risebrobakken et al., 2003; Andersson et al., 2003) suggest an increased influence of AW in the eastern Nordic seas throughout the last 3000 yr. The correspondence between our *G. muellerae* abundance datasets and foraminiferal records is particularly obvious in core HH11-134-BC off western Svalbard, where foraminifera are assumed to represent subsurface waters within the main core of Atlantic-derived waters (Carstens et al., 1997), thus confirming the reliability of this coccolith index as a proxy of Atlantic water flow.

The following discussion compares our data with previous marine and terrestrial proxy records of sea ice distribution, atmospheric circulation (NAO index), and sea surface and subsurface temperatures in the northern North Atlantic region in order to provide a thorough insight into the paleoceanographical and paleoclimatological development of this climatic sensitive area during the late Holocene. In the final part we will zoom in on the major climatic changes during the last 700 yr covering the interval from the MCA–LIA transition to the modern period.

4.3.1 Reconciling the observed long-term trends in AW flow and distribution of surface waters with the so-called "neoglacial cooling"

The manifestation of the late Holocene (last ∼ 3000 yr) trend toward positive NAO conditions can be inferred from various marine proxy records around Greenland showing colder conditions associated with decreased AW influence in Discobay (western Greenland) related to the so-called "seesaw" pattern (Seidenkrantz et al., 2008; Andresen et al., 2011, 2012), and an increased flux of sea ice/icebergs east of Greenland (Jennings et al., 2002). Accordingly, Moros et al. (2004) interpreted the patterns of increased abundance of ice-rafted detritus (IRD) in the western parts of the Nordic Seas (Jennings et al., 2002) and decreased IRD in the Norwegian Sea (their work) to a strengthening of both the NAC and the EGC from the mid-Holocene to present. This coupled strengthened circulation affecting the eastern and western parts of the Nordic Seas is consistent with modern observations (Blindheim et al., 2000; Furevik and Nilsen, 2005) and modeling experiments (Nilsen et al., 2003), which relate it to atmospheric processes akin to the present positive
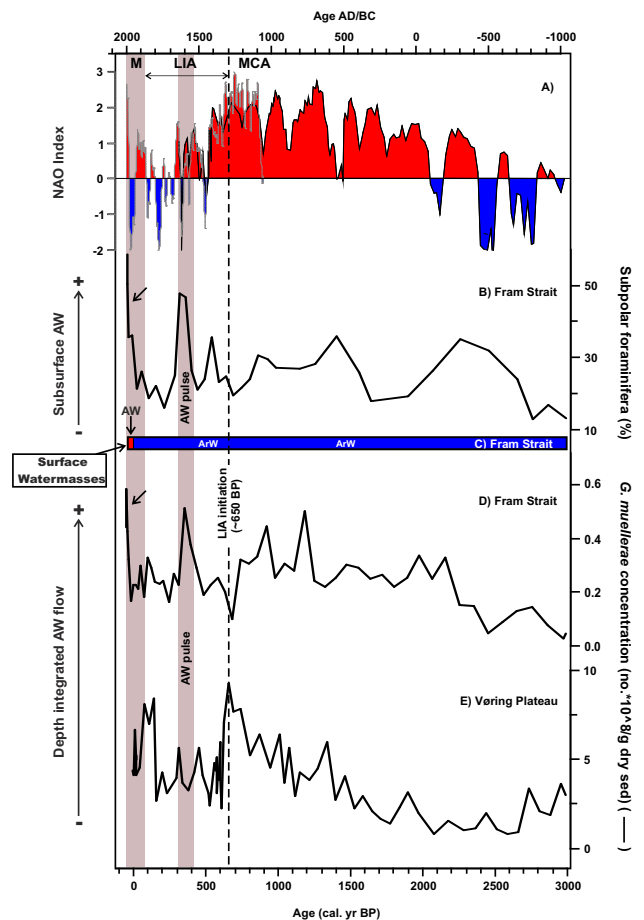

Fig. 7. Summary plot of surface and subsurface circulation changes across the eastern Nordic Seas over the past 3000 yr. **(A)** Combined NAO index reconstruction based on Trouet et al. (2009) and Olsen et al. (2012); red area represents positive NAO and blue area negative NAO conditions. **(B)** Relative abundance of subpolar foraminifera (fraction > 100 μm) at site HH11-134-BC as an index of subsurface AW masses. **(C)** Dominating surface water masses at site HH11-134-BC (Fram Strait) inferred from E/C ratios. **(D)** **(E)** Dynamics of AW flow off western Svalbard (top) and off western Norway (bottom) inferred from absolute concentrations of the AW inflow species *G. muellerae*. The grey shaded areas indicate the marked inflow increases during the modern period and the intra-LIA event centered at 330–410 cal yr BP. The dashed, thick line refers to the initiation of the LIA according to Miller et al. (2012).

phase of the NAO. Finally, a strengthening of the NAC and its WSC extension has earlier been suggested by Sarnthein et al. (2003) based on a general increase in reconstructed subsurface temperatures in the western Barents Sea, which the authors related to a slight increase of the thermohaline circulation (THC). Concurrent glacier expansions on west Spitsbergen (Svendsen and Mangerud, 1997) and increased winter precipitation over mid-western Norway (Nesje et al., 2001) throughout the last 3000 yr additionally argue for strengthened southwesterlies and an associated increase in NAC and

WSC flows, related to the increasingly positive NAO trend, which together constitute the main source of moisture for these high latitude regions.

The surface water expression of the inferred strengthened AW flow toward the northern Nordic Seas is marked by an overall trend of increased influence of surface AW masses in the western Barents Sea and off western Svalbard (Fig. 5). Sustained surface AW conditions occurred earlier at site JM09-KA11-GC from ca. 1000 cal yr BP than at the northernmost Fram Strait site HH11-134-BC where poleward AW due to the overall dominating sea ice conditions (last 3000 yr; Müller et al., 2012) did not affect the surface until the last century. The increased flow of the WSC branch of the NAC throughout the late Holocene has previously been suggested from planktonic foraminiferal-based SST reconstructions off western Barents Sea (Sarnthein et al., 2003) as well as from phytoplankton biomarkers and $CaCO_3$ contents in sediments off western Svalbard (Müller et al., 2012), to which our coccolith proxy (E / C ratio) of surface water masses might further add some constrains and improve the understanding of changes in the water column distribution of AW in the northern North Atlantic.

The studied site off western Norway shows an opposite surface signature to the northernmost locations (Fig. 5): here, though always overlaid by the surface AW mass over the last 3000 yr, core MD95-2011 displays a decreasing E / C ratio, most prominently during the last 1200 yr (increase in *C. pelagicus*), which translates into an increasing proximity to ArW. Once again, modern observations on the influence of NAO upon the surface hydrology of the eastern Nordic Seas might shed light on this apparent paradox. Instrumental records are indeed indicative of a correlation between changes in the NAO index and surface temperature variations (Blindheim et al., 2000; Miettinen et al., 2011), which is stronger west of Svalbard than off western Norway (Blindheim et al., 2000). Strengthened westerlies (positive NAO index) (Fig. 7), whose track of maximum wind stress in the eastern Nordic Seas affects the oceanic area off south and mid-Norway, force both an increased flow of AW and a narrowing of the surface expression of the NAC toward the Norwegian slope (Blindheim and Østerhus, 2005; and references herein). An obvious implication at MD95-2011 is an increased proximity of arctic-derived surface water (eastward shift of the AF), throughout the last 3000 yr, as suggested by the trend of coccolith E / C ratio (Fig. 5), and confirmed by Norwegian Sea diatom- (Andersen et al., 2004; Birks and Koç, 2002) and alkenone-derived SST reconstructions (Calvo et al., 2002).

4.3.2 Zooming in on the Little Ice Age and the modern period. Time interval ∼ 700–0 cal yr BP

The late Holocene trend of increased poleward flow of AW was interrupted by a sudden shift to a period of deteriorating conditions that we assume corresponds to the MCA–LIA

transition (Fig. 7). The slight offset in the timing of the observed LIA initiation between the stratigraphically best resolved core MD95-2011 (ie. ca. 660 cal yr BP) and the two northernmost locations can to a large extent be explained by the use in the present study of a standard reservoir correction ($R = 0$) to constrain the stratigraphical framework of all three studied sediment cores, a simplification that does not take into account possible varying contribution of "old" carbon from Arctic/Polar water masses off western Svalbard and the western Barents Sea . The MCA–LIA climatic shift is thought to have been triggered by a combination of a reduction in solar irradiance, explosive volcanism and changes in the internal modes of variability of the ocean–atmosphere system, as one single process cannot usually explain this cold period alone (Wanner et al., 2011). The suggested 660 cal yr BP MCA–LIA age lies within the range of previously proposed ages for the initiation of this climate deterioration in the studied region (Hald et al., 2011; Sejrup et al., 2011), and closely corresponds to recent evidences from Arctic Canada and Iceland (Miller et al., 2012) for a 50 yr long explosive volcanism centered at 650 cal yr BP. According to these latter authors, the onset of the LIA was directly linked to such volcanic events that triggered an extensive sea ice expansion causing a self-sustaining sea ice/ocean feedback until modern times. As volcanic eruptions seems to modify on short timescales a naturally occurring variability mode similar to the NAO toward its positive phase (Graf et al., 1993), the reconstructed major change to a negative NAO index across the MCA–LIA transition (Fig. 7; Olsen et al., 2012) is most likely related to other forcings i.e., greenhouse gasses, stratospheric ozone and solar irradiance (Gillett et al., 2003). Nevertheless such a concomitant change in the NAO pattern from a long-term positive phase to highly fluctuating negative NAO conditions around 640 cal yr BP (Fig. 7a) possibly additionally contributed to an increase in sea ice extent, as decadal and long-term variations in large-scale ice concentrations has shown to be significantly correlated with long-term NAO variations (Visbeck et al., 2003). This major change in turn impacted the efficiency of the NAC flow to the northern North Atlantic (Fig. 7d), therefore further maintaining, if not strengthening, the sea ice expansion across the northern Nordic seas (Werner et al., 2011; Müller et al., 2012).

The harsh LIA conditions favored colder surface and subsurface waters in the eastern Fram Strait as also reflected by the E / C ratio and planktonic foraminiferal abundance patterns in core HH11-134BC (Fig. 7b, c). The prevailing Arctic/Polar surface water masses in the eastern Fram Strait stands however as a strong contrast to the dominating surface signature of AW at the western Barents Sea core site (Fig. 5). The specific location of core JM09-KA11-GC within the influence of both AW (WSC) and ArW (Sørkapp Current, Bear Island Current) suggests that although sea ice cover was probably enhanced over the western Barents Sea during this climate deterioration, this local area was affected by a highly

fluctuating sea ice boundary with strong seasonal gradients characterized by an early spring break up of the winter sea ice, and a strong spring/early summer stratification and AW dominance during summer (favoring *E. huxleyi*). The specific surface expression at this site is further confirmed by the overall similarities between our E/C proxy (JM09-KA11-GC) and reconstructed atmospheric temperatures from a lake record in western Svalbard (D'Andrea et al., 2012), an area influenced by similar hydrological features (e.g., sea ice, the Sørkapp Current and the WSC). D'Andrea et al. (2012) identified a temperature increase starting at ∼ 1600 AD over western Svalbard as well as mild LIA summer conditions, which they explained by a strengthened WSC (NAC), a strengthening only inferred in the present study from our JM09-KA11-GC coccolith record. We therefore suggest the identified warming on Svalbard to be rather due to a decreased flow of polar waters over the shelf via the Sørkapp Current and the Bear Island Current, rather than changes in the strength of the NAC, possibly resulting in a seasonally stronger AW influence on atmospheric temperatures and sea ice extent.

The above described Arctic/Polar LIA conditions in the eastern Fram Strait was interrupted by a sudden short pulse of increased WSC flow between ∼ 330 and 410 cal yr BP as depicted in HH11-134-BC by our *G. muellerae* proxy records (Fig. 7b, d) as well as a maximum in subpolar foraminiferal abundance. This strengthened, short-lived AW flow to the northern Nordic Seas was synchronous with a short-term increase in the Atlantic Multi-decadal Oscillation (Gray et al., 2004; Winter et al., 2011) and a change towards positive NAO phases. Both processes are likely to explain the minimum sea ice anomaly in the Nordic Seas during the 15th century, compared with the previous and later centuries, as evidenced by Macias-Fauria et al. (2009) and Kinnard et al. (2011). The magnitude of this warm pulse, as evidenced by our coccolith proxy record, falls within the range of the AW flow strengthening during the MCA, and is only surpassed by the maximum in AW flow during the modern period (Fig. 7d).

The reconstructions on Arctic sea ice by Kinnard et al. (2011) are particularly coherent with the message given by the *G. muellerae* concentrations at core HH11-134-BC with a phasing of the WSC flow pulse and the following deteriorating conditions in both AW flow (our work) and sea ice extent until the early 20th century (Kinnard et al., 2011), suggesting a generally strong impact of AW flow dynamics on the Arctic sea ice extent.

The LIA cool climatic period was reversed during the 19th century by an overall increase in atmospheric and sea temperatures, as reconstructed from marine and terrestrial high resolution proxy records from the Arctic region (Overpeck et al., 1997; Kaufman et al., 2009). Recent studies on sea surface temperature reconstructions over the last 2000 yr in the Malangen Fjord, northwestern Norway (Hald et al., 2011), and west of Spitsbergen (Spielhagen et al., 2011),

and evidences herein of high amplitude, rapid temperature increases during the last century, has intensified the ongoing debate on temperature changes in the Arctic. Spielhagen et al. (2011) used foraminiferal assemblages and geochemical measurements to reconstruct a ∼ 2 °C temperature increase in the subsurface waters of the eastern Fram Strait at the transition from the LIA to the modern period. Our dataset obtained from core HH11-134-BC not only confirms the high amplitude warming of subsurface waters at the turn of the 19th century (Fig. 7), it also shows that such a warming was primarily induced by an excess flow of AW along western Svalbard as depicted by our *G. muellerae* proxy record (Fig. 7d). Our coccolith results also indicates that this modern strengthening of AW flow across Fram Strait was unprecedented over the last 3000 yr, and was associated by an exceptional AW shoaling (Fig. 7c), in agreement with reported historical lows in sea ice extent in the Nordic Seas since the second half of the 19th century (Divine and Dick, 2006).

5 Conclusions

Late Holocene changes in the flow of AW and in the nature of surface waters along the eastern border of the Nordic Seas are reconstructed from coccolith proxy records distributed from the mid-western Norwegian margin to the eastern Fram Strait. Our floral records show a general strengthened NAC flow from 3000 cal yr BP to the present, which affected the whole investigated latitudinal range from 66 to 77° N. This long-term modulation in the AW flow appeared linked to atmospheric processes driven by dominant modes of NAO. This mechanism also explains the observed zonal shifts in the location of the AF off western Norway, with increased influence of ArW during strengthened westerlies (positive NAO mode), whereas the western Barents Sea and eastern Fram Strait experienced an overall shoaling of AW that is proportional to its integrated flow to this northernmost settings.

The Little Ice Age, which according to our best-dated records, initiated at ∼ 660 cal yr BP, is seen as an episode of deteriorating conditions, with Arctic/Polar surface waters off western Svalbard and the western Barents Sea, possibly associated with severe sea ice conditions, and a strongly reduced AW flow. This strong cooling was interrupted in the eastern Fram Strait by a short resumed high flow of WSC from ca. 330 to 410 cal yr BP, whose magnitude was only surpassed by the one that characterizes the modern period.

Our dataset not only confirms the high amplitude warming of surface waters at the turn of the 19th century off western Svalbard, it also shows that such a warming was primarily induced by an excess flow of AW, which stands as unprecedented over the last 3000 yr.

The publication of this article
is financed by CNRS-INSU.

References

Andersen, C., Koc, N., Jennings, A., and Andrews, J. T.: Non-uniform response of the major surface currents in the Nordic Seas to insolation forcing: Implications for the Holocene climate variability, Paleoceanography, 19, PA2003, doi:10.1029/2002PA000873, 2004.

Andersson, C., Risebrobakken, B., Jansen, E., and Dahl, S. O.: Late Holocene surface ocean conditions of the Norwegian Sea (Vøring Plateau), Paleoceanography, 18, PA1044, doi:10.1029/2001PA000654, 2003.

Andresen, C. S., McCarthy, D. J., Dylmer, C. V., Seidenkrantz, M.-S., Kuijpers, A., and Lloyd, J. M.: Interaction between subsurface ocean waters and calving of the Jakobshavn Isbræ during the late Holocene, Holocene, 21, 211–224, 2011.

Andresen, C. S., Hansen, M. J., Seidenkrantz, M-S., Jennings, A. E., Knudsen, M. F., Nørgaard-Pedersen, N., Larsen, N. K., Kuijpers, A., and Pearce, C.: Mid- to late-Holocene oceanographic variability on the Southeast Greenland shelf, Holocene, 23, 167–178, 2012.

Andrews, J. T. and Giraudeau, J.: Multi-proxy records showing significant Holocene variability: the inner N. Iceland shelf (Húnaflói), Quaternary Sci. Rev., 22, 175–193, 2003.

Andruleit, H.: A filtration technique for quantitative studies of coccoliths, Mar. Micropaleontol., 42, 403–406, 1996.

Andruleit, H.: Coccolithophore fluxes in the Norwegian-Greenland Sea: Seasonality and assemblage alterations, Mar. Micropaleontol., 31, 45–64, 1997.

Andruleit, H. and Baumann, K.-H.: History of the last deglaciation and Holocene in the Nordic Seas as revealed by coccolithophore assemblages, Mar. Micropaleontol., 35, 179–201, 1998.

Baumann, K.-H., Andruleit, H., and Samtleben, C.: Coccolithophores in the Nordic Seas: Comparison of living communities with surface sediment assemblages, Deep-Sea Res. Pt. II, 47, 1743–1772, 2000.

Beaufort, L. and Heussner, S.: Seasonal dynamics of calcareous nannoplankton on a West European continental margin: the Bay of Biscay, Mar. Micropaleontol., 43, 27–55, 2001.

Berben, S., Husum, K., Cabedo-Sanz, P., and Belt, S.: Holocene sub centennial evolution of Atlantic water inflow and sea ice distribution in the western Barents Sea, in preparation, 2013.

Birks, C. J. A. and Koç, N.: A high-resolution diatom record of late-Quaternary sea-surface temperatures and oceanographic conditions from the eastern Norwegian Sea, Boreas, 31, 323–344, 2002.

Bjune, A. E., Seppä, H., and Birks, H. J. B.: Quantitative summer-temperature reconstructions for the last 2000 yr based on pollen-stratigraphical data from northern Fennoscandia, J. Paleolimnol., 41, 43–56, 2009.

Blindheim, J. and Østerhus, S.: The Nordic seas, main oceanographic features, in: The Nordic Seas: an integrated perspective Oceanography, Climatology, Biochemistry, and Modelling, edited by: Drange, H., Dokken, T., Furevik, T., Gerdes, R., and Berger, W., Geophys. Monogr. Ser., 158, 11–37, 2005.

Blindheim, J., Borovkov, V., Hansen, B., Malmberg, S. Aa., Turrell, W. R., and Østerhus, S.: Upper layer cooling and freshening in the Norwegian Sea in relation to atmospheric forcing, Deep-Sea Res. Pt. I, 47, 655–680, 2000.

Buch, E.: A monograph on the physical oceanography of the Greenland waters, Danish Meteorological Institute Scientific Report 00-12, Greenland Fisheries Research Insitute publication 15 series, 0-244, 1990.

Cachão, M. and Moita, M. T.: Coccolithus pelagicus, a productivity proxy related to moderate fronts off Western Iberia, Mar. Micropaleontol., 39, 131–155, 2000.

Calvo, E., Grimalt, J., and Jansen, E.: High resolution U^k_{37} sea surface temperature reconstruction in the Norwegian Sea during the Holocene, Quaternary Sci. Rev., 21, 1385–1394, 2002.

Carstens, J., Hebbeln, D., and Wefer, G.: Distribution of planktic foraminifera at the ice margin in the Arctic (Fram Strait), Mar. Micropaleontol., 29, 257–269, 1997.

Cronin, T. M., Thunell, R., Dwyer, G. S., Saenger, C., Mann, M. E., Vann, C., and Seal, R. R.: Multiproxy evidence of Holocene climate variability from estuarine sediments, eastern North America, Paleoceanography, 20, PA4006, doi:10.1029/2005PA001145, 2005.

D'Andrea, W. J., Vaillencourt, D. A., Balascio, N. L., Werner, A., Roof, S. R., Reteller, M., and Bradley, R. S.: Mild Little Ice Age and unprecedented recent warmth in an 800 year lake sediment record from Svalbard, Geology, 40, P1007, doi:10.1130/G33365.1, 2012.

Divine, D. V. and Dick, C.: Historical variability of sea ice edge position in the Nordic Seas, J. Geophys. Res., 111, CO1001, doi:10.1029/2004JC002851, 2006.

Duplessy, J.-C., Ivanova, E., Murdmaa, I., Paterne, M., and Labeyrie, L.: Holocene paleoceanography of the northern Barents Sea and variations of the northward heat transport by the Atlantic Ocean, Boreas, 30, 2–16, 2001.

Dylmer, C. V., Giraudeau, J., Hanquiez, V., and Husum, K.: The coccolithophores Emiliania Huxleyi and Coccolithus pelagicus: extant populations from the Norwegian-Iceland Sea and Fram Strait, in preparation, 2013.

Furevik, T. and Nilsen, J. E. Ø.: Large-Scale Atmospheric Circulation Variability and its Impacts on the Nordic Seas Ocean Cli-

mate – A Review, Geophys. Monogr. Ser., 158, 105–136, 2005.

Gillett, N. P., Graf, H. F., and Osborn, T. J.: Climate Change and the North Atlantic Oscillation, AGU Geophys. Monogr., 134, in: The North Atlantic Oscillation: Climatic Significance and Environmental Impact, edited by: Hurrell, J. W., Kushnir, Y., Ottersen, G., and Visbeck, M., American Geophysical Union, Washington, DC, 1–36, 2003.

Giraudeau, J., Grelaud, M., Solignac, S., Andrews, J. T., Moros, M., and Jansen, E.: Millenial-scale variability in Atlantic water advection to the Nordic Seas derived from Holocene coccolith concentration records, Quaternary Sci. Rev., 29, 1276–1287, 2010.

Graf, H. F., Perlwitz, J., and Kirchner, I.: Northern Hemisphere tropospheric mid-latitude circulation after violent volcanic eruptions, report no. 107, Max-Planck-Institut füur Meteorologie, Hamburg, 1–18, 1993.

Gray, S. T., Graumlich, L. J., Betancourt, J. L., and Pederson, G. T.: A tree-ring based reconstruction of the Atlantic Multidecadal Oscillation since 1567 A.D., Geophys. Res. Lett., 31, L12205, doi:10.1029/2004GL019932, 2004.

Groot, D. E., Sørensen, S. Aa., and Husum, K.: Holocene Atlantic Water inflow to the western Barents Sea margin, in preparation, 2013.

Hald, M., Andersson, C., Ebbesen, H., Jansen, E., Klitgaard-Kristensen, D., Risebrobakken, B., Salomonsen, G. R., Sarnthein, M., Sejrup, H. P., and Telford, R. J.: Variations in temperature and extent of Atlantic Water in the northern North Atlantic during the Holocene, Quaternary Sci. Rev., 26, 3423–3440, 2007.

Hald, M., Salomonsen, G. R., Husum, K., and Wilson, L. J.: A 2000 year record of Atlantic Water temperature variability from the Malangen Fjord, northeastern North Atlantic, Holocene, 21, 1049–1059, 2011.

Hansen, B. and Østerhus, S.: North-Atlantic-Nordic Seas exchanges, Prog. Oceanogr., 45, 109–208, 2000.

Hebbeln, D., Henrich, R., and Baumann, K. -H.: Paleoceanography of the Last Interglacial/ Glacial Cycle in the Polar North Atlantic, Quaternary Sci. Rev., 17, 125–153, 1998.

Herrle, J. O. and Bollmann, J.: Accuracy and reproducibility of absolute nannoplankton abundances using filtration techniques in combination with a rotary splitter, Mar. Micropaleontol., 53, 389–404, 2004.

Hopkins, T. S.: The GIN sea – a synthesis of its physical oceanography and literature review 1972–1985, Earth-Sci. Rev., 30, 175–318, 1991.

Hurrell, J. W.: Decadal trends in the North Atlantic Oscillation: Regional temperatures and precipitation, Science, 269, 676–679, 1995.

Hurrell, J. W., Kushnir, Y., Ottersen, G., and Visbeck, M.: An overview of the North Atlantic Oscillation, AGU Geophys. Monogr., 134, in: The North Atlantic Oscillation: Climatic Significance and Environmental Impact, edited by: Hurrell, J. W., Kushnir, Y., Ottersen, G., and Visbeck, M., American Geophysical Union, Washington, DC, 1–36, 2003.

Husum, K. and Hald, M.: Arctic planktic foraminiferal assemblages: Implications for subsurface temperature reconstructions, Mar. Micropaleontol., 96–97, 38–47, 2012.

Jennings, A. E., Knudsen, K. L., Hald, M., Hansen, C. V., and Andrews, J. T.: A mid-Holocene shift in Arctic sea-ice variability on the East Greenland Shelf, Holocene, 12, 49–58, 2002.

Kaufman, D. S., Schneider, D. P., Mckay, N. P., Ammann, C. M., Bradley, R. S., Briffa, K. R., Miller, G. H., Otto-Bliesner, B. L., Overpeck, J. T., and Vinther, B. M., Arctic Lakes 2k Projekt members: Recent warming reverses long-term Arctic cooling, Science, 325, 1236–1239, 2009.

Kinnard, C., Zdanowicz, C. M., Fisher, D. A., Isaksson, E., de Vernal, A., and Thompson, L. G.: Reconstructed changes in Arctic sea ice over the past 1.450 years, Nature, 479, 509–512, 2011.

Kwok, R., Cunningham, G. F., and Pang, S. S.: Fram Strait sea-ice outflow, J. Geophys. Res., 109, C01009, doi:10.1029/2003JC001785, 2004.

Lund, D. C., Lynch-Stieglitz, J., and Curry, W. B.: Gulf Stream density structure and transport during the past millenium, Nat. Lett., 444, 601–604, 2006.

Macias-Faria, M., Grinsted, A., Helama, S., Moore, J., Timonen, M., Martma, T., Isaksson, E., and Eronen, M.: Unprecedented low twentieth century winter sea-ice extent in the Western Nordic Seas since A.D. 1200, Clim. Dynam., 34, 781–795, 2009.

Marshall, J., Kushnir, Y., Battisti, D., Chang, P., Czaja, A., Dickson, R., Hurrell, J., McCartney, M., Saravanan, R., and Visbeck, M.: North Atlantic Climate Variability: Phenomena impacts and mechanisms, Int. J. Climatol., 21, 1863–1898, 2001.

Matthiessen, J., Baumann, K. H., Schröder-Ritzrau, A., Hass, C., Andruleit, H., Baumann, A., Jensen, S., Kohly, A., Pflaumann, U., Samtleben, C., Schäfer, P., and Thiede, J.: Distribution of calcareous, siliceous and organic-walled planktic microfossils in surface sediments of the Nordic Seas and their relation to surface-water masses, in: The northern North Atlantic: a changing environment, edited by: Schäfer, P., Ritzrau, W., Schlüter, M., and Thiede, J., Springer-Verlag, Berlin, 105–127, 2001.

Miettinen, A., Koç, N., Hall, I. R., Godtliebsen, F., and Divine, D.: North Atlantic sea surface temperatures and their relation to the North Atlantic Oscillation during the last 230 years, Clim. Dynam., 36, 533–543, 2011.

Miller, G. H., Geirsdòttir, A., Zhong, Y., Larsen, D. J., Otto-Bliesner, B. L., Holland, M. M., Bailey, D. A., Refsnider, K. A., Lehman, S. J., Southon, J. R., Anderson, C., Björnsson, H., and Thordarson, T.: Abrupt onset of the Little Ice Age triggered by volcanism and sustained by sea-ice/ocean feedbacks, Geophys. Res. Lett., 39, L02708, doi:10.1029/2011GL050168, 2012.

Moros, M., Emeis, K., Risebrobakken, B., Snowball, I., Kuijpers, A., McManus, J., and Jansen, E.: Sea surface temperatures and ice rafting in the Holocene North Atlantic: Climate influences on northern Europe and Greenland, Quaternary Sci. Rev., 23, 2113–2126, 2004.

Müller, J., Werner, K., Stein, R., Fahl, K., Moros, M., and Jansen, E.: Holocene cooling culminates in sea-ice oscillations in Fram Strait, Quaternary Sci. Rev., 47, 1–14, 2012.

Nesje, A., Kvamme, M., Rye, N., and Løvlie, R.: Holocene glacial and climate history of the Jostedalsbreen region, western Norway; evidence from lake sediments and terrestrial deposits, Quaternary Sci. Rev., 10, 87–114, 1991.

Nesje, A., Matthews, J. A., Dahl, S. O., Berrisford, M. S., and Andersson, C.: Holocene glacier fluctuations of Flatebreen and winter-precipitation changes in the Jostedalsbreen region, western Norway, based on glaciolacustrine sediment records, Holocene, 11, 267–280, 2001.

Nilsen, J. E. Ø., Gao, Y., Drange, H., Furevik, T., and Bentsen, M.: Simulated North Atlantic-Nordic Seas water mass exchanges in

an isopycnic coordinate OGCM, Geophys. Res. Lett., 30, 1536, doi:10.1029/2002GL016597, 2003.

Olsen, J., Anderson, N. J., and Knudsen, M. F.: Variability of the North Atlantic Oscillation over the last 5,200 years, Nat. Geosci., 5, 808–812, 2012.

Overpeck, J., Hughen, K., Hardy, D., Bradley, R., Case, R., Douglas, M., Finney, B., Gajewski, K., Jacoby, G., Jennings, A., Lamoureux, S., Lasca, A., MacDonald, G., Moore, J., Retelle, M., Smith, S., Wolfe, A., and Zielinski, G.: Arctic environmental change of the last four centuries, Science, 278, 1251–1256, 1997.

Porter, S. C. and Denton, G. H.: Chronology of neoglaciation in the North American Cordillera, Am. J. Sci., 265, 177–210, 1967.

Reimer, P. J.: IntCal09 and Marine09 radiocarbon age calibration curves, 0–50,000 years cal BP, Radiocarbon, 51, 1111–1150, 2009.

Risebrobakken, B., Jansen, E., Andersson, C., Mjelde, E., and Hevrøy, K.: A high-resolution study of Holocene paleoclimatic and paleoceanographic changes in the Nordic Seas, Paleoceanography, 18, PA1017, doi:10.1029/2002PA000764, 2003.

Risebrobakken, B., Moros, M., Ivanova, E. V., Chistyakova, N., and Rosenberg, R.: Climate and oceanographic variability in the SW Barents Sea during the Holocene, Holocene, 20, 609–621, 2010.

Rüther, D. C., Bjarnadòttir, L. R., Junttila, J., Husum, K., Rasmussen, T. L., Lucchi, R. G., and Andreassen, K.: Pattern and timing of the northwestern Barents Sea Ice Sheet deglaciation and indications of episodic Holocene deposition, Boreas, 41, 494–512, 2012

Saloranta, T. M. and Svendsen, H.: Across the Arctic front west of Spitsbergen: high-resolution CTD sections from 1998–2000, Polar Res., 20, 177–184, 2001.

Samtleben, C. and Schröder, A.: Living cocolithophore communities in the Norwegian-Greenland Sea and their record in sediments, Mar. Micropaleontol., 19, 333–354, 1992.

Samtleben, C., Schäfer, P., Andruleit, H., Baumann, A., Baumann, K. H., Kohly, A., Matthiessen, J., and Schröder-Ritzrau, A.: Plankton in the Norwegian-Greenland Sea: from living communities to sediment assemblages – an actualistic approach, Geol. Rundsch., 84, 108–136, 1995.

Sarnthein, M., Van Kreveld, S., Erlenkeuser, H., Grootes, P. M., Kucera, M., Pflaumann, U., and Schulz, M.: Centennial-to-millennial-scale periodicities of Holocene climate and sediment injections off the western Barents shelf, Boreas, 32, 447–461, 2003.

Schröder-Ritzrau, A., Andruleit, H., Jensen, S., Samtleben, C., Schäfer, P., Matthiessen, J., Hass, C., Kohly, A., and Thiede, J.: Distribution, export and alteration of fossilizable plankton in the Nordic Seas, in: The Northern North Atlantic: A Changing Environment, edited by: Schäfer, P., Ritzrau, W., Schlüter, M., and Thiede, J., Springer, Berlin, 81–104, 2001.

Seidenkrantz, M.-S., Roncaglia, L., Fischel, A., Heilmann-Clausen, C., Kuijpers, A., and Moros, M.: Variable North Atlantic climate seesaw patterns documented by a late Holocene marine record from Disko Bugt, West Greenland, Mar. Micropaleontol., 68, 66–83, 2008.

Sejrup, H. P., Haflidason, H., and Andrews, J. T.: A Holocene North Atlantic SST record and regional climate variability, Quaternary Sci. Rev., 30, 3181–3195, 2011.

Skagseth, Ø., Furevik, T., Ingvaldsen, R., Loeng, H., Mork, K. A., Orvik, K. A., and Ozhigin, V.: Volume and heat transports to the Arctic Ocean via the Norwegian and Barents Seas, in: Arctic-Subarctic Ocean Fluxes: Defining the role of the Northern Seas in Climate, edited by: Dickson, R., Meincke, J., and Rhines, P., Springer Netherlands, 25–64, 2008.

Sorteberg, A. and Kvingedal B.: Atmospheric forcing on the Barents Sea Winter Ice Extent, J. Climate, 19, 4772–4784, 2006.

Spielhagen, R. F., Werner, K., Aagaard-Sørensen, S., Zamelczyk, K., Kandiano, E., Budeus, G., Husum, K., Marchitto, T. M., and Hald, M.: Enhanced modern heat transfer to the Arctic by Warm Atlantic Water, Science, 331, 450–453, 2011.

Stuiver, M. and Reimer, P. J.: Extended ^{14}C data base and revised CALIB 3.0 ^{14}C age calibration program, Radiocarbon, 35, 215–230, 1993.

Svendsen, J. I. and Mangerud, J.: Holocene glacial and climatic variations on Spitsbergen, Svalbard, Holocene, 7, 45–57, 1997.

Trouet, V., Esper, J., Graham, N. E., Baker, A., Scourse, J. D., and Frank, D. C.: Persistent positive North Atlantic Oscillation mode dominated the Medieval Climate Anomaly, Science, 324, 78–80, 2009.

Vinje, T.: Anomalies and trends of sea-ice extent and atmospheric circulation in the Nordic Seas during the period 1864–1998, J. Climate, 14, 255–267, 2001.

Visbeck, M., Chassignet, E. P., Curry, R. G., Delworth, T. L., Dickson, R. R., and Krahmann, G.: The Ocean's response to North Atlantic Oscillation variability, AGU Geophys. Monogr., 134, in: The North Atlantic Oscillation: Climatic Significance and Environmental Impact, edited by: Hurrell, J. W., Kushnir, Y., Ottersen, G., and Visbeck, M., American Geophysical Union, Washington, D. C., 113–146, 2003.

Wanamaker Jr., A. D., Butle, P. G., Scourse, J. D., Heinemeie, J., Eiríksson, J., Knudsen, K. L., and Richardson, C. A.: Surface changes in the North Atlantic meridional overturning circulation during the last millenium, Nat. Commun., 3, 899, doi:10.1038/ncomms1901, 2012.

Wanner, H., Solomina, O., Grosjean, M., Ritz, S. P., and Jetel, M.: Structure and origine of Holocene cold events, Quaternary Sci. Rev., 30, 3109–3123, 2011.

Wassmann, P., Reigstad, M., Haug, T., Rudels, B., Carroll, M. L., Hop, H., Gabrielsen, G. W., Falk-Petersen, S., Denisenko, S. G., Arashkevich, E., Slagstad, D., and Pavlova, O.: Food webs and carbon flux in the Barents Sea, Prog. Oceanogr., 71, 232–287, 2006.

Werner, K., Spielhagen, R. F., Bauch, D., Hass, H. C., Kandiano, E., and Zamelczyk, K.: Atlantic Water advection to the eastern Fram Strait – Multiproxy evidence for late Holocene varibility, Palaeogeogr. Palaeocl., 308, 264–276, 2011.

Wilson, L. J., Hald, M., and Godtliebsen, F.: Foraminiferal faunal evidence of twentieth-century Barents Sea warming, Holocene, 21, 527–537, 2011.

Winter, A., Miller, T., Kushnir, Y., Sinha, A., Timmermann, A., Jury, M. R., Gallup, C., Cheng, H., and Edwards, R. L.: Evidence for 800 years of North Atlantic multi-decadal variability from a Puerto Rican speleothem, Earth Planet. Sc. Lett., 308, 23–28, 2011.

Ziveri, P., Kleijne, A., Conte, M., and Weber, J.: Coccolithophorid distribution and alkenone biomarker characterisation from the tropical Equatorial Atlantic, European Geophysical Society (EGS), Nice, XXVI General Assembly, 2001.